NSS

Neutrosophic Sets and Systems, Vol. 98, 2026

University of New Mexico

Soft Clustering Technique for Brain Tumor Segmentation within Neutrosophic Framework

Nandhini Mohan[1], Dhanalakshmi Palanisami[1,*] and Lavanya Ganeshkumar[1]

[1]Department of Applied Mathematics, Bharathiar University, Coimbatore - 641046, India.

[*]Correspondence: dhanamath@buc.edu.in

Abstract. Precise segmentation of brain tumors is vital in healthcare because it impacts diagnosis, treatment planning, and patient outcomes. However, the brain has complex structures with non-linear and inhomogeneous forms, which poses substantial challenges for conventional segmentation approaches. Despite of intensive research works, there persists a need to improve segmentation accuracy while concurrently lowering the computing costs. To address this, this study presents an innovative segmentation framework that incorporates kernel distance into the neutrosophic c-means (NCM) algorithm, together with the Kullback-Leibler (KL) divergence measure. Furthermore, the integration of kernel distance enables the algorithm to adeptly identify non-linear structural fluctuations and eliminate outliers, which improves robustness. Besides, the KL divergence mechanism accelerates convergence and improves segmentation precision by increasing the clustering process by reducing the distance between neighbourhood membership degrees. The proposed approach has been assessed against five established clustering algorithms utilizing both objective performance metrics and subjective visual evaluations. Experimental findings validate that the proposed method attains enhanced accuracy with increased computational efficiency and more precise delineation of tumor areas. Additionally, these results underscore the potential of the developed method for brain tumor segmentation, helping to bridge existing methodological gaps and promote more efficient medical image analysis.

Keywords: Medical image segmentation; Uncertainty; Neutrosophic set; Kernel distance; KL divergence

1. Introduction

Tumors are abnormal growth of the tissues that appear in various regions of the body which affect normal physiological activities and cause major risks to health [1]. Depending upon the nature, they can be classified as benign or malignant, that are distinguished by their aggressive and invasive behaviour. Among these, brain tumors are the most serious threat due to their ability to disrupt fundamental neurological functioning, which can lead to severe

health consequences. Therefore, early discovery and precise characterisation of brain tumors are essential for determining viable treatment techniques, such as surgery, radiotherapy, and chemotherapy, that can significantly improve patient outcomes. Brain tumors, which can grow from the brain tissue or metastasise from other regions of the human body, which makes the medical imaging and diagnosis a challenging task. Further, It is laborious to precisely identify and characterise tumour locations due to the very sensitive and complex nature of brain tissues combined with the variability in tumor morphology and behaviour. In that context, physicians make use variety of imaging modalities to capture the brain for better diagnosis and treatment process. Among which, magnetic resonance imaging (MRI) become the more significant for diagnosing and evaluating brain tumors due to its superior contrast resolution and ability to provide detailed images of soft tissues [2]. It enables to visualize the different types of tissues in the brain and aids to detect the even subtle abnormalities in the brain. In addition, MRI enables the physicians to examine the characteristics of tumor such as size, its involvement in surrounding tissues and its location through offering variety of sequences such as T1-weighted, T2-weighted and fluid attenuated inversion recovery images.

Despite the advantages of MRI, the manual segmentation of brain tumors from MRI scans remains a time-consuming and intensive process, subject to inter- and intra-observer variability. This has led to increased research efforts toward automated brain tumor segmentation methods, which aim to accurately and efficiently segment tumors from MRI images [3]. Thus, wide range of researchers contributed to this domain by developing the variety of algorithms based on thresholding [4], region growing [5], water-shed, [6] and clustering based techniques [7]. Apart from all other approaches, clustering based techniques have gained attention for their ability to group image pixels with similar characteristics in an unsupervised manner, without requiring large labelled datasets which aids in effective separation of tumor regions from healthy regions into distinct clusters based on intensity, texture and spatial information. Moreover, clustering algorithms can be categorised into hard [7] and soft clustering approaches. Hard clustering methods includes k-means clustering [8], mean shift clustering [9] etc., but these clustering techniques are unable to handle data points that belong to multiple clusters leading to inaccurate segmentation.

Unlike hard clustering, soft clustering techniques [10] includes fuzzy c-means clustering (FCM), probabilistic clustering etc., allows pixels to belong multiple clusters with different degrees of belongingness, which is useful to efficiently deal with the complex, non-linear structures. At first, Bezdek introduced the FCM clustering approach that allows the data pints to have different degree of membership in more than one cluster [11]. This approach efficiently segments the brain image than hard clustering approaches by handling the uncertainties in the images. Followed by this work, to improve the performance of the clustering and extend

it in various fields, many researchers developed the advanced variants of FCM to handle the multi-modal datas. Particularly, many refined variants of FCM is introduced to cluster the brain images by efficiently handling the uncertainties and improve the performance through the use of difference distance measures and so on [12]- [14]. In addition, as the extension of this technique, type-2 fuzzy based FCM is developed to deal with noise and imprecise date with complex structures by improving the flexibility in membership modelling. Further, intuitionistic fuzzy c-means clustering (IFCM) is formulated that advances the traditional FCM techniques by incorporating the degrees of membership, non-membership and hesitation [15]. This approach improved the cluster separation and providing the more nuanced representation. Furthermore, kernel distance is replaced the Euclidean distance in IFCM to form the kernel induced FCM (KIFCM) method to deal with the non-linear data [16].

While fuzzy sets are effective in handling uncertainty in medical images, there remains a need for enhanced capabilities to address complex, structured, and uncertain medical images. The neutrosophic set (NS) [17] framework builds upon traditional fuzzy sets by effectively managing indeterminacy and extending their applicability to these challenging scenarios. Based on this, Guo and Sengur formulated the neutrosophic c-means clustering (NCM) by adopting degree of determinacy, indeterminacy and falsity in the objective function providing a more comprehensive approach to representing various uncertainty [18]. Moreover, this algorithm introduces two kinds of rejection which are outlier rejection and noise rejection for effective segmentation. Further, Akubulut et al., authors extend NCM for clustering nonlinear-shaped data by integrating a kernel function, creating a new algorithm called kernel neutrosophic c-means (KNCM) [19]. Subsequently, Singh et al., developed the type-2 NS to cluster the images through the information obtained from the neutrosophic entropy [20]. While clustering algorithms aspire for greater accuracy, they frequently result in longer runtimes and increased computational complexity. This highlights the critical need of efficiency optimisation for these algorithms. Thus, to speed up this optimisation, it is possible to use the local spatial information included inside brain images. Based on this, Gharieb and Gendy (LMKLFCM), modified the criterion function of FCM by incorporating the KL information distance. This algorithm promotes the alignment of the cluster membership of a pixel with the smoothed membership functions of its local neighbourhood by minimising the KL distance [21, 22]. Also, this procedure provides robustness against noise and generates clustered images with piecewise homogeneous regions. At a subsequent time Lu et al., [23] formulated the NKWNLICM method by inculcating the noisy distance and fuzzy spatial information into the NCM technique to enhance the performance of image segmentation. Thereafter, Wang et al., devised the segmentation technique based on KL divergence integrated with wavelet transforms and morphological reconstruction (KLDFCM) to improve the efficiency [24]. Following this, Kumar et al., devised the clustering

process (FBkPC_S1) by integrating the FCM objective function to bounded cluster planes and adds the local spatial information to the criterion function to handle the noise efficiently [25]. Then, Farooq and Memon developed the clustering algorithm by making use of kernel metric with possibilistic FCM to reduce the computational cost [26].

Even though, the significant researches has been done on this domain, still brain tumor segmentation persists the challenging task due to various aspects. First, the structural complexity of the brain is a formidable barrier and the tumor region has the overlapping boundaries, complex structures and heterogeneous intensity distributions of the brain. Due to these reasons, the conventional techniques often prone to over-segmentation and under-segmentation, which results in inaccurate representation of tumor regions. Second, MRI images are prone to noise, motion and acquisition artifacts which further leads to higher risk of misclassification. Furthermore, the lack of sufficient contrast between tumor and its surrounding tissues increases the complexity in accurate determination of boundaries, particularly in early-stages of tumors. Another major limitation lies in the sensitivity of clustering algorithms to initialization and outliers. Most conventional c-means and its variants converge to local optima, where initial centroid placement strongly influences the final clustering result. Even though, existing fuzzy and neutrosophic approaches effective in modelling uncertainty but often fail to capture non-linear structures when restricted to Euclidean distance, which leads to the loss of critical anatomical details. These limitations are further evident when applied to complex brain regions, resulting in higher computational costs and reduced efficiency.

In light of above mentioned challenges , this research sets out to refine a clustering technique in an effort to minimise computational cost while simultaneously enhancing the level of accuracy of the segmented result by effectively handling noise, low contrast and structural complexity. By addressing these limitations, a new clustering algorithm is proposed by integrating the kernel distance metric and KL divergence term into the objective function of NCM (KLKNCM). Kernel distance metric aids to cluster the non-linear structures present the brain images which improves the accuracy of the segmented result. Meanwhile, the KL divergence term helps to reduce the noise and improve similarity identification between data points and cluster centres that preserves neighbourhood relationships. Further, it fastens the convergence of the algorithm which in result reduces the computational cost of the proposed clustering technique. Additionally, the efficiency of the proposed algorithm is tested against state-of-the-art techniques and evaluated through both objective and subjective assessments. The key contributions of the proposed KLKNCM algorithm are outlined as follows:

(1) A novel clustering algorithm, termed KLKNCM is introduced. By embedding the kernel distance metric within the neutrosophic c-means formulation, the proposed framework effectively captures non-linear structural variations in brain images, enabling superior

tumor delineation compared to conventional clustering methods. The inclusion of the KL divergence term strengthens the similarity assessment between data points and cluster centers. This preserves spatial neighbourhood relationships, reduces the effect of noise, and enhances intra-cluster compactness and inter-cluster separability.

(2) The algorithm incorporates mechanisms to identify and suppress the influence of outliers, thereby enhancing segmentation robustness. Through the incorporation of the KL divergence term and fuzzy membership assignment, anomalous or noisy pixels receive diminished membership weights, thereby minimizing their influence on cluster formation. This ensures reliable segmentation even in the presence of noise and artifacts.

(3) By utilising the joint benefits of kernel distance and KL divergence, the KLKNCM algorithm achieves faster convergence with fewer iterations, thereby lowering the computational cost relative to existing clustering techniques.

Additionally, the structure of this manuscript is as follows: Section 2 presents the background study, which serves as the primary motivation for this work. Section 3 outlines the proposed KLKNCM technique. Next, Section 4 describes the experimental setup, followed by Section 5 which offers a comprehensive assessment of the study. Finally, the conclusions are drawn in Section 8.

2. **Background Works**

2.1. *NCM*

Consider an image represented by set of pixels and let it be $K = \{k_1, k_2, \ldots, k_a | a = 1, 2, \ldots, N\}$ where k_a represents the intensity a^{th} pixel in the image and N corresponds to the total number of pixels in the image. Let C be the total number of clusters into which the image has to be segmented and each cluster has its own centre which is symbolised as c_b. Then, the optimization function for NCM is given as follows.

$$\begin{aligned} min\, \mathcal{L}_{NCM}(\mathcal{T}, \mathcal{I}, \mathcal{F}, \mathcal{C}) = & \sum_{a=1}^{N}\sum_{b=1}^{C}(\mathcal{Z}_1\mathcal{T}_{ab})^m \|k_a - w_b\|^2 + \sum_{a=1}^{N}(\mathcal{Z}_2\mathcal{I}_a)^m \|k_a - \bar{w}_{a_{max}}\|^2 + \sum_{a=1}^{N}\xi^2(\mathcal{Z}_3\mathcal{F}_a)^m \\ \text{subject to} \quad & \sum_{b=1}^{C}\mathcal{T}_{ab} + \mathcal{I}_a + \mathcal{F}_a = 1, 1 \leq a \leq N. \end{aligned} \tag{1}$$

Here, $\bar{w}_{a_{max}} = \dfrac{w_{e_i} + w_{f_i}}{2}$ and $e_i = \underset{b=1,2,\ldots C}{\arg\max}(\mathcal{T}_{ab})$, $f_i = \underset{b \neq e_{a \cap b}=1,2,\ldots C}{\arg\max}(\mathcal{T}_{ab})$.

In the above give objective function (1), T_{ab} indicates the degree of belongingness of the determinant cluster, whereas, I_a and F_a represents the degree of membership of the boundaries and outlier clusters with $0 < T_{ab}, I_a, F_a < 1$ satisfying the given constraint in the objective function. Moreover, e_i and f_i defines to the cluster numbers corresponding to the first largest and the second largest value of T_{ab} and its average value is signified as $\bar{w}_{a_{max}}$. Moreover, $\mathcal{Z}_i$, $i = 1, 2, 3$

characterises the weight factor for the d determinant, indeterminant and outlier degrees and ξ denotes the outlier control parameter which is used for identifying and managing outliers, reducing their influence on cluster formation, and enhancing the algorithm's robustness to noise and anomalies. It enables fine-tuning of the algorithm's sensitivity to outliers, leading to more accurate and reliable clustering, particularly in complex datasets with noise or uncertainty.

The criterion function is minimized by utilising the Lagrangian multiplier and then it is solved to obtain the degree of membership and the centroid of each cluster. Accordingly, the degree of determinant, boundaries and the outliers are obtained as given in the equation outlined below.

$$\mathcal{T}_{ab} = \frac{P}{\mathcal{Z}_1}(k_a - w_b)^{-(2/m-1)} \tag{2}$$

$$\mathcal{I}_a = \frac{P}{\mathcal{Z}_2}(k_a - \bar{w_a}_{\max})^{-(2/m-1)} \tag{3}$$

$$\mathcal{F}_a = \frac{P}{\mathcal{Z}_3}\xi^{-(2/m-1)} \tag{4}$$

Subsequently, the centroid for the each cluster is deduced as expressed in the equation (5),

$$v_j = \frac{\sum_{a=1}^{N}(\mathcal{Z}_1\mathcal{T}_{ab})^m k_a}{\sum_{a=1}^{N}(\mathcal{Z}_1\mathcal{T}_{ab})^m} \tag{5}$$

where $P = \left(\frac{\lambda_i}{m}\right)^{1/m-1}$ such that λ_i is Lagrangian constant. Moreover, during each iteration of the clustering process, the membership values and cluster centres are updated, and the objective function is minimised in order to segment the image. Significantly, the decision-making process does not explicitly consider the membership degrees of boundary and outliers. The method stops when the absolute difference between consecutive iterations of $\mathcal{T}_{ab}$ values is less than a specified threshold δ, or when the maximum number of iterations is reached.

2.2. *LMKLFCM Technique*

This technique incorporates the KL divergence to the objective function of FCM clustering to make the clustering process computationally efficient with better result. In this process the inclusion of the KL divergence component ensures that the membership grades of a given image pixel become substantially similar to those of its neighbours. As a consequence, optimising the membership partition during each iteration improves the segmentation performance of the algorithm. In addition, minimising the KL distance allows the labelling of a pixel to be impacted by its neighbours which leads to the development of piecewise homogeneous regions inside the image, concurrently providing an efficient approach for reducing the noise in the

image. The criterion function for the LMKLFCM technique is given in equation (6).

$$\begin{aligned} \min \mathcal{L}_{\text{LMKLFCM}} &= \sum_{a=1}^{N}\sum_{b=1}^{C}\mu_{ab}\|k_a - w_b\|^2 + \lambda\sum_{a=1}^{N}\sum_{b=1}^{C}\mu_{ab}\log\frac{\mu_{ab}}{\pi_{ab}} \\ \text{subject to} \quad & \sum_{b=1}^{C}\mu_{ab} = 1, 1 \le a \le N. \end{aligned} \tag{6}$$

In the above equation, π_{ab} indicates the moving membership average function, which is computed by averaging the memberships μ_{ab} across a neighbourhood window that is centred around μ_{ij} within n space, represented as N_n. Mathematically, the moving average function is given as, $\pi_{ab} = \dfrac{1}{N_j}\sum\limits_{j\in N_n}\mu_{aj}$. Further, μ_{ab} indicates the membership degree of the a^{th} data point in the b^{th} cluster and the second part in the objective function symbolises the KL divergence distance. Moreover, the other terms specified in the equation (6) are described in the previous subsection. Following this, the membership degree and the centroid of each cluster are determined by integrating the Lagrangian multiplier into the objective function and optimising it through minimisation. Consequently, the equations presented below delineate the degree of membership (8) and centroid (7) for each cluster of the LMKLFCM technique.

$$w_b = \frac{\sum_{a=1}^{N}\mu_{ab}\,k_a}{\sum_{a=1}^{N}\mu_{ab}} \tag{7}$$

$$\mu_{ab} = \frac{\pi_{ab}\exp^{-(\|k_a - w_b\|^2)/\lambda}}{\sum_{b=1}^{C}\pi_{aj}\exp^{-(\|k_a - w_j\|^2)}} \tag{8}$$

In turn, the LMKLFCM technique systematically segments the image by optimizing the criterion function and iteratively refining the membership values μ_{ab} associated with the centroid of the each cluster. Finally, the iteration process wraps up when the absolute difference between successive iterations of the μ_{ab} values falls below a particular termination criterion, denoted as δ, or when the maximum number of iterations is reached.

3. **Proposed KLKNCM Technique**

Motivated by the works give in the preceding section and to improve the accuracy of the segmented images. The KLKNCM technique has been developed to improve the segmentation of brain images, focusing on enhancing accuracy while simultaneously minimising computation cost. This is achieved by integrating the kernel function and the KL divergence measure into the criterion function. The integration of the kernel function is imperative for precisely recognising the non-linear structures present within the inhomogeneous regions of the brain. Further, it facilitates the mapping of input data into a higher-dimensional feature space, which improves the capacity of the algorithm to identify complex patterns and boundaries that may not be simply separable within the original input space. Thus, incorporating the kernel function is beneficial for segmenting the intricate and inhomogeneous images to attain precise delineation.

Further, KL divergence helps to lower noise by encouraging consistency among adjacent pixels and improve similarity identification between data points and cluster centres that preserves neighbourhood relationships. Also, KL divergence improves segmentation accuracy, accelerates convergence, reduces computational cost, and enables the flexible management of imbalanced data distributions due to its non-symmetric nature. Through inculcating these two metrics in proposed method effectively captures intricate image patterns, resulting in more precise segmentation results while preserving computational efficiency. Hence, the criterion function for the proposed method is mathematically expressed as in equation (9).

$$min\,\mathcal{L}_{\mathrm{KLKNCM}}(T,I,F,C)=\sum_{a=1}^{N}\sum_{b=1}^{C}(\mathcal{Z}_1\mathcal{T}_{ab})\|\psi(k_a)-\psi(w_b)\|^2+\sum_{a=1}^{N}(\mathcal{Z}_2\mathcal{I}_a)\|\psi(k_a)-\psi(\bar{w}_{a_{\max}})\|^2+\sum_{a=1}^{N}\xi^2(\mathcal{Z}_3\mathcal{F}_a)+D(T,I,F,\bar{T},\bar{I},\bar{F}) \tag{9}$$

where, D indicates the KL divergence measure and it is defined as follows,

$$D(T,I,F,\bar{T},\bar{I},\bar{F})=\sum_{a=1}^{N}\sum_{b=1}^{C}\mathcal{T}_{ab}\log\frac{\mathcal{T}_{ab}}{\bar{\mathcal{T}}_{ab}}+\sum_{a=1}^{N}\mathcal{I}_a\log\frac{\mathcal{I}_a}{\bar{\mathcal{I}}_a}+\sum_{a=1}^{N}\mathcal{F}_a\log\frac{\mathcal{F}_a}{\bar{\mathcal{F}}_a} \tag{10}$$

and $(D)\to 0$. The median filter applied on the degree of belongingness of determinate, boundary, and outliers using the chosen window size which is symbolised as $\bar{\mathcal{T}}_{ab},\bar{\mathcal{I}}_a,\bar{\mathcal{F}}_a$ respectively. Thereafter, the criterion function of the proposed techniques is modified as given below.

$$\begin{aligned}\min\ \mathcal{L}_{\mathrm{KLKNCM}}(T,I,F,C)=&\sum_{a=1}^{N}\sum_{b=1}^{C}(\mathcal{Z}_1\mathcal{T}_{ab})\|\psi(k_a)-\psi(w_b)\|^2+\sum_{a=1}^{N}(\mathcal{Z}_2\mathcal{I}_a)\|\psi(k_a)-\psi(\bar{w}_{a_{\max}})\|^2\\&+\sum_{a=1}^{N}\xi^2(\mathcal{Z}_3\mathcal{F}_a)+\gamma\left(\sum_{a=1}^{N}\sum_{b=1}^{C}\mathcal{T}_{ab}\log\frac{\mathcal{T}_{ab}}{\bar{\mathcal{T}}_{ab}}+\sum_{a=1}^{N}\mathcal{I}_a\log\frac{\mathcal{I}_a}{\bar{\mathcal{I}}_a}+\sum_{a=1}^{N}\mathcal{F}_a\log\frac{\mathcal{F}_a}{\bar{\mathcal{F}}_a}\right)\\\text{subject to}\quad&\sum_{b=1}^{C}\mathcal{T}_{ab}+\mathcal{I}_a+\mathcal{F}_b=1,1\le a\le N.\end{aligned} \tag{11}$$

The kernel induced distance is expressed as,

$$\|\psi(k_a)-\psi(w_b)\|^2=\mathcal{K}(k_a,k_a)-2\mathcal{K}(k_a,w_b)+\mathcal{K}(w_b,w_b) \tag{12}$$

In this work, the Gaussian kernel is used as the kernel function. Hence it known that $\mathcal{K}(k_a,k_a)=\mathcal{K}(w_b,w_b)=1$ and the above equation is deduced as equation (14) and (15) receptively.

$$\|\psi(k_a)-\psi(w_b)\|^2=2(1-\mathcal{K}(k_a,w_b)) \tag{13}$$

similarly,

$$\|\psi(k_a)-\psi(\bar{w}_{a_{\max}})\|^2=2(1-\mathcal{K}(k_a,\bar{w}_{a_{\max}})) \tag{14}$$

Thus, substituting the equations (14) and (15) to the (11). Therefore, the transformed final objective function is given as in equation (15).

$$\begin{aligned}\min \mathcal{L}_{\mathrm{KLKNCM}}(T,I,F,C) =& 2\sum_{a=1}^{N}\sum_{b=1}^{C}(\mathcal{Z}_1\mathcal{T}_{ab})(1-\mathcal{K}(k_a,w_b)) + 2\sum_{a=1}^{N}(\mathcal{Z}_2\mathcal{I}_a)(1-\mathcal{K}(k_a,\bar{w}_{a_{\max}})) \\ &+ \sum_{a=1}^{N}\xi^2(\mathcal{Z}_3\mathcal{F}_a) + \gamma\left(\sum_{a=1}^{N}\sum_{b=1}^{C}\mathcal{T}_{ab}\log\frac{\mathcal{T}_{ab}}{\bar{\mathcal{T}}_{ab}} + \sum_{a=1}^{N}\mathcal{I}_a\log\frac{\mathcal{I}_a}{\bar{\mathcal{I}}_a} + \sum_{a=1}^{N}\mathcal{F}_a\log\frac{\mathcal{F}_a}{\bar{\mathcal{F}}_a}\right) \\ \text{subject to} \quad & \sum_{b=1}^{C}\mathcal{T}_{ab} + \mathcal{I}_a + \mathcal{F}_b = 1, 1 \le a \le N.\end{aligned} \tag{15}$$

In the preceding equation, $\mathcal{Z}_i$ indicates the weight factor, whereas ξ refers to outlier control parameter. Further, the positive parameter γ influences the objective function by controlling the consequences of the KL divergence term. As the subsequent process, the proposed objective function is minimised by incorporating the Lagrangian multiplier in it. Mathematically, the Lagrangian inculcated criterion function is formulated as given below.

$$\begin{aligned}\mathcal{L}(T,I,F,C) =& 2\sum_{a=1}^{N}\sum_{b=1}^{C}(\mathcal{Z}_1\mathcal{T}_{ab})(1-\mathcal{K}(k_a,w_b)) + 2\sum_{a=1}^{N}(\mathcal{Z}_2\mathcal{I}_a)(1-\mathcal{K}(k_a,\bar{w}_{a_{\max}})) \\ &+ \sum_{a=1}^{N}\xi^2(\mathcal{Z}_3\mathcal{F}_a) + \gamma\left(\sum_{a=1}^{N}\sum_{b=1}^{C}\mathcal{T}_{ab}\log\frac{\mathcal{T}_{ab}}{\bar{\mathcal{T}}_{ab}} + \sum_{a=1}^{N}\mathcal{I}_a\log\frac{\mathcal{I}_a}{\bar{\mathcal{I}}_a} + \sum_{a=1}^{N}\mathcal{F}_a\log\frac{\mathcal{F}_a}{\bar{\mathcal{F}}_a}\right) \\ &- \sum_{a=1}^{N}\lambda_a\left(\sum_{b=1}^{C}\mathcal{T}_{ab} + \mathcal{I}_a + \mathcal{F}_a - 1\right)\end{aligned} \tag{16}$$

Thus, to minimize the above given objective function, partial derivative of the objective function with respect to the membership degree of determinate, boundary, outlier points and the cluster centre are computed and it presented in equations (17)-(19).

$$\frac{\partial L}{\partial \mathcal{T}_{ab}} = 2\mathcal{Z}_1(1-\mathcal{K}(k_a,w_b)) + \gamma\left(\log\frac{\mathcal{T}_{ab}}{\bar{\mathcal{T}}_{ab}} + 1\right) - \lambda_a \tag{17}$$

$$\frac{\partial L}{\partial \mathcal{I}_a} = 2\mathcal{Z}_2(1-\mathcal{K}(k_a,\bar{w}_{a_{\max}})) + \gamma\left(\log\frac{\mathcal{I}_a}{\bar{\mathcal{I}}_a} + 1\right) - \lambda_a \tag{18}$$

$$\frac{\partial L}{\partial \mathcal{F}_a} = \xi^2\mathcal{Z}_3 + \gamma\left(\log\frac{\mathcal{F}_a}{\bar{\mathcal{F}}_a} + 1\right) - \lambda_a \tag{19}$$

Let $\frac{\partial L}{\partial \mathcal{T}_{ab}} = 0$, $\frac{\partial L}{\partial \mathcal{I}_a} = 0$, and $\frac{\partial L}{\partial \mathcal{F}_a} = 0$, then solving the equations(17), (18), (19) yields

$$\mathcal{T}_{ab} = \exp^{\frac{\lambda_a}{\gamma}} . \exp^{\frac{\gamma(log(\bar{\mathcal{T}}_{ab})-1)-2\mathcal{Z}_1(1-\mathcal{K}(k_a,w_b))}{\gamma}} \tag{20}$$

$$\mathcal{I}_a = \exp^{\frac{\lambda_a}{\gamma}} . \exp^{\frac{\gamma(log(\bar{\mathcal{I}}_a)-1)-2\mathcal{Z}_2(1-\mathcal{K}(k_a,\bar{w}_{a_{\max}}))}{\gamma}} \tag{21}$$

$$\mathcal{F}_a = \exp^{\frac{\lambda_a}{\gamma}} . \exp^{\frac{\gamma(log(\bar{\mathcal{F}}_a)-1)-\xi\mathcal{Z}_3}{\gamma}} \tag{22}$$

Let $\exp^{\frac{\lambda_a}{\gamma}} = A$ and the objective function is constrained to $\sum_{b=1}^{C} \mathcal{T}_{ab} + \mathcal{I}_a + \mathcal{F}_a = 1$, then

$$A\left[\exp^{\frac{\gamma(log(\bar{\mathcal{T}}_{ab})-1)-2\mathcal{Z}_1(1-\mathcal{K}(k_a,w_b))}{\gamma}} + \exp^{\frac{\gamma(log(\bar{\mathcal{I}}_a)-1)-2\mathcal{Z}_2(1-\mathcal{K}(k_a,\bar{w_a}_{\max}))}{\gamma}} + \exp^{\frac{\gamma(log(\bar{\mathcal{F}}_a)-1)-\xi\mathcal{Z}_3}{\gamma}}\right] = 1 \tag{23}$$

$$A = \left[\exp^{\frac{\gamma(log(\bar{\mathcal{T}}_{ab})-1)-2\mathcal{Z}_1(1-\mathcal{K}(k_a,w_b))}{\gamma}} + \exp^{\frac{\gamma(log(\bar{\mathcal{I}}_a)-1)-2\mathcal{Z}_2(1-\mathcal{K}(k_a,\bar{w_a}_{\max}))}{\gamma}} + \exp^{\frac{\gamma(log(\bar{\mathcal{F}}_a)-1)-\xi\mathcal{Z}_3}{\gamma}}\right]^{-1} \tag{24}$$

Finally, the degree of membership for determinate, indeterminate, and ouliers are formulated as follows,

$$\mathcal{T}_{ab} = A\ \exp^{\frac{\gamma(log(\bar{\mathcal{T}}_{ab})-1)-2\mathcal{Z}_1(1-\mathcal{K}(k_a,w_b))}{\gamma}} \tag{25}$$

$$\mathcal{I}_a = A.\exp^{\frac{\gamma(log(\bar{\mathcal{I}}_a)-1)-2\mathcal{Z}_2(1-\mathcal{K}(k_a,\bar{w_a}_{\max}))}{\gamma}} \tag{26}$$

$$\mathcal{F}_a = A.\exp^{\frac{\gamma(log(\bar{\mathcal{F}}_a)-1)-\xi\mathcal{Z}_3}{\gamma}} \tag{27}$$

Furthermore, to calculate the centroid for each cluster, the Gaussian kernel ($G(k_a, w_a)$) induced objective function is given as

$$\begin{aligned}\mathcal{L}(T,I,F,C) =& 2\sum_{a=1}^{N}\sum_{b=1}^{C}(\mathcal{Z}_1\mathcal{T}_{ab})(1-\exp\left(\frac{-\|k_a,w_b\|}{\sigma^2}\right) + 2\sum_{a=1}^{N}(\mathcal{Z}_2\mathcal{I}_a)(1-\exp\left(\frac{-\|k_a,\bar{w_a}_{\max}\|}{\sigma^2}\right)\\ &+\sum_{a=1}^{N}\xi^2(\mathcal{Z}_3\mathcal{F}_a) + \gamma\left(\sum_{a=1}^{N}\sum_{b=1}^{C}\mathcal{T}_{ab}\log\frac{\mathcal{T}_{ab}}{\bar{\mathcal{T}}_{ab}} + \sum_{a=1}^{N}\mathcal{I}_a\log\frac{\mathcal{I}_a}{\bar{\mathcal{I}}_a} + \sum_{a=1}^{N}\mathcal{F}_a\log\frac{\mathcal{F}_a}{\bar{\mathcal{F}}_a}\right)\\ &-\sum_{a=1}^{N}\lambda_a\left(\sum_{b=1}^{C}\mathcal{T}_{ab}+\mathcal{I}_a+\mathcal{F}_a-1\right)\end{aligned} \tag{28}$$

Taking the first derivative of the above equation with respect to w_b and equating it to zero. The following expression is deduced.

$$w_b = \frac{\sum_{a=1}^{N}(\mathcal{Z}_1\mathcal{T}_{ab})G(k_a,w_b)k_a}{\sum_{a=1}^{N}(\mathcal{Z}_1\mathcal{T}_{ab})G(k_a,w_a)} \tag{29}$$

The minimization of the criterion function is achieved by iterating the defined steps until convergence is reached and the membership degrees and cluster centers are updated for each iteration. Convergence is determined when the absolute difference between the values of T_{ab} from two consecutive iterations falls below a specified termination criterion δ, or when the maximum number of iterations is attained. Moreover, the parameters such as $\mathcal{Z}_i$, ξ and γ plays an crucial role in the clustering process. Hence, the analysis for the values chosen for the parameters will be given in succeeding section and the computational algorithm for the proposed technique is provided in the Algorithm 1.

Algorithm 1 Formulation of proposed KLKNCM alogrithm

Require: Number of cluster centre (C), weight factors ($\mathcal{Z}_1, \mathcal{Z}_2, \mathcal{Z}_3$), outlier controller ($\xi$), KL parameter ($\gamma$), terminating criterion (δ), .

Step 1: Initialize $\mathcal{T}_{ab}^{(0)}$, $\mathcal{I}_a^{(0)}$ and $\mathcal{F}_a^{(0)}$.

Step 2: $y \leftarrow 1$

Step 3: ***repeat***

Step 4: Calculate $w_b^{(h)}$ using (29).

Step 5: Compute $\bar{w_a}_{\max}^{(h)}$.

Step 6: Update $\mathcal{T}_{ab}^{(h)}$, $\mathcal{I}_a^{(h)}$ and $\mathcal{F}_a^{(h)}$ using (25)-(27) and the objective function given in Eq (16).

Step 7: $y \leftarrow y + 1$

Step 8: ***until*** $|\mathcal{T}_{ab}^{(h+1)} - \mathcal{T}_{ab}^{(h)}| < \delta$ or $h \geq h_{max}$.

Step 9: ***return*** w_b, $T = \{\mathcal{T}_{ab}\}_{C\times N}$ and the iteration count h.

4. Experimental Details

The present section outlines the experimental framework of the proposed technique, providing detailed information on the dataset utilized in this study. Additionally, it discusses the comparative clustering algorithms and the clustering validation metrics employed to evaluate the performance of the KLKNCM technique.

4.1. *Description of the Dataset and Comparative Clustering Methods*

It is known that the brain, a highly intricate and structurally complex organ, presents significant challenges for image segmentation algorithms. Thus, to evaluate the performance of the proposed KLKNCM algorithm, brain images were selected for analysis. For this purpose, the BraTS (Brain Tumour Segmentation) dataset was employed [27], which is a benchmark for the segmentation of brain tumors. This dataset includes images of brains affected by glioblastoma, an aggressive and malignant form of brain cancer, in which T1-weighted MRI images were used for the clustering process because they have more detailed anatomy, which is important for accurately capturing the complexity of brain structures in segmentation tasks. Moreover, the use of this dataset enables a comprehensive assessment of the algorithm's capability to handle complex and heterogeneous medical images.

To assess the effectiveness and superiority of the proposed KLKNCM technique, a comparison analysis is performed against many cutting-edge clustering algorithms. In this sense, five clustering algorithms were chosen based on important characteristics pertinent to the study's scope. The NCM-1 [18], NCM-2 [28] and KNCM [19] algorithms were included due to the reason that they have integrated NS theory into the soft clustering framework, which is essential for managing indeterminate and incomplete information. Moreover, in order to evaluate the influence of spatial information on clustering, KLDFCM [24] and FBkPC_S1 [25] were

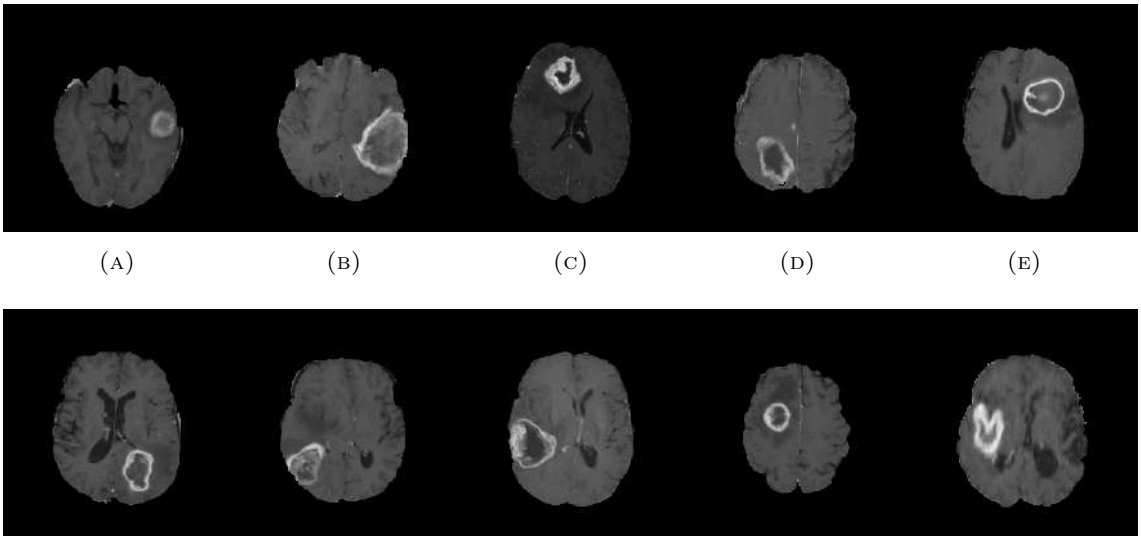

(A) (B) (C) (D) (E)

(F) (G) (H) (I) (J)

FIGURE 1. Source images adopted for the experiment.

selected, as these methods incorporate spatial features to improve clustering accuracy. The NKWNLICM [23] technique was chosen because it combines NS theory with local information clustering mechanisms, resulting in spatially aware clustering. Furthermore, it is worth noting that the parameters of each comparative method were carefully changed to fit the issue formulation in the current study, ensuring a fair and objective comparison of performance across all methods.

4.2. *Cluster Validation Metrics*

In order to evaluate the results in quantitative aspects, the clustering validation metrics is utilised. These metrics offers the valuable insights of the final clustered results obtained from the proposed and other comparative clustering techniques in various aspect. Thus, the metric encompassed in this work is described below. Moreover, the experiment is executed in MATLAB R2019a software and to maintain the preciseness and presentation, the results from ten images are analysed and discussed in the paper.

(1) **Fuzzy Performance Index (FPI)**

FPI [31] is used to assess the effectiveness and quality of the clustering, particularly it quantifies the compactness of the clusters. Mathematically it is represented as in equation (30).

$$FPI = 1 - \frac{C}{C-1}(1 - F_c) \tag{30}$$

where, F_c is the partition coefficient and it is calculated as $F_c = \frac{1}{N}\sum_{a=1}^{N}\sum_{b=1}^{C}(\mathcal{T}_{ab})^2$.

(2) **Modified Partition Entropy (MPE)**

MPE [31] evaluates the degree of overlap and intersections and uncertainty among the clusters. It is calculated using the following formula.

$$MPE = \frac{N.PE}{N - C} \tag{31}$$

such that, $PE = -\frac{1}{N}\sum_{a=1}^{N}\sum_{b=1}^{C}[\mathcal{T}_{ab} log_2(\mathcal{T}_{ab})^2]$ is the partition entropy. Lower the value indicates the better clustered result.

(3) **Xie-Beni Index (XBI)**

XBI [31] is the effective tool to ensure the quality of compactness and well-separated clusters of the resultant images. Further, it is calculated as follows,

$$XBI = \frac{\sum_{a=1}^{N}\sum_{b=1}^{C}\mathcal{T}_{ab}^2 x^2(k_a, w_b)}{N(\min_{i\neq b} x^2(w_i, w_b))} \tag{32}$$

where k_a refers the values of the pixel and w_b indicated the centroid of the cluster. Moreover, the lower the values of this metric represents the better outcome.

5. Analysis of Parameters

A detailed parameter analysis was conducted to evaluate the impact of various algorithmic parameters in the performance of the proposed method. By systematically adjusting key parameters, such as weighting parameters, weight factors ($\mathcal{Z}_1, \mathcal{Z}_2, \mathcal{Z}_3$), outlier controller ($\xi$), KL parameter ($\gamma$), terminating criterion (δ), number of cluster centre (C), the optimal configuration for the proposed method was determined. Further, the results of the parameter analysis demonstrated that fine-tuning these parameters leads to significant improvements in both the precision of the segmented regions and the overall stability of the clustering process. In this clustering analysis, three weight factors $\mathcal{Z}_1, \mathcal{Z}_2$ and $\mathcal{Z}_3$ are assigned values of 0.8, 0.1, and 0.1, respectively. These weights control the influence of different features in the clustering process, where $\mathcal{Z}_1$ is the most dominant, and $\mathcal{Z}_2$ and $\mathcal{Z}_3$ contribute less significantly to decrease the influence of outliers. Then the optimal value of ξ for better clustering result is ranges from 140 to 200 for the considered dataset. Another key parameter is σ ranging from $[0.3, 0.8]$. Further, for improved segmented result, the value of γ is analysed and it varies from 10000 to 15000. Added to this, the image is segmented into four region and hence the centroid of the cluster C fixed as 4. Finally, the terminating value δ is set to 0.0001. This detailed examination provides insights into the sensitivity of the proposed method to different parameter values, ensuring that the algorithm outperforms consistently.

6. Experimental Analysis

This section provides a thorough evaluation of the proposed method, incorporating both objective and subjective assessments to benchmark its performance against other state-of-the-art techniques. The objective assessment delivers a quantitative evaluation, focusing on metrics such as segmentation accuracy, precision, computational efficiency, and runtime. Meanwhile, the subjective assessment offers a qualitative comparison, emphasizing the visual quality of

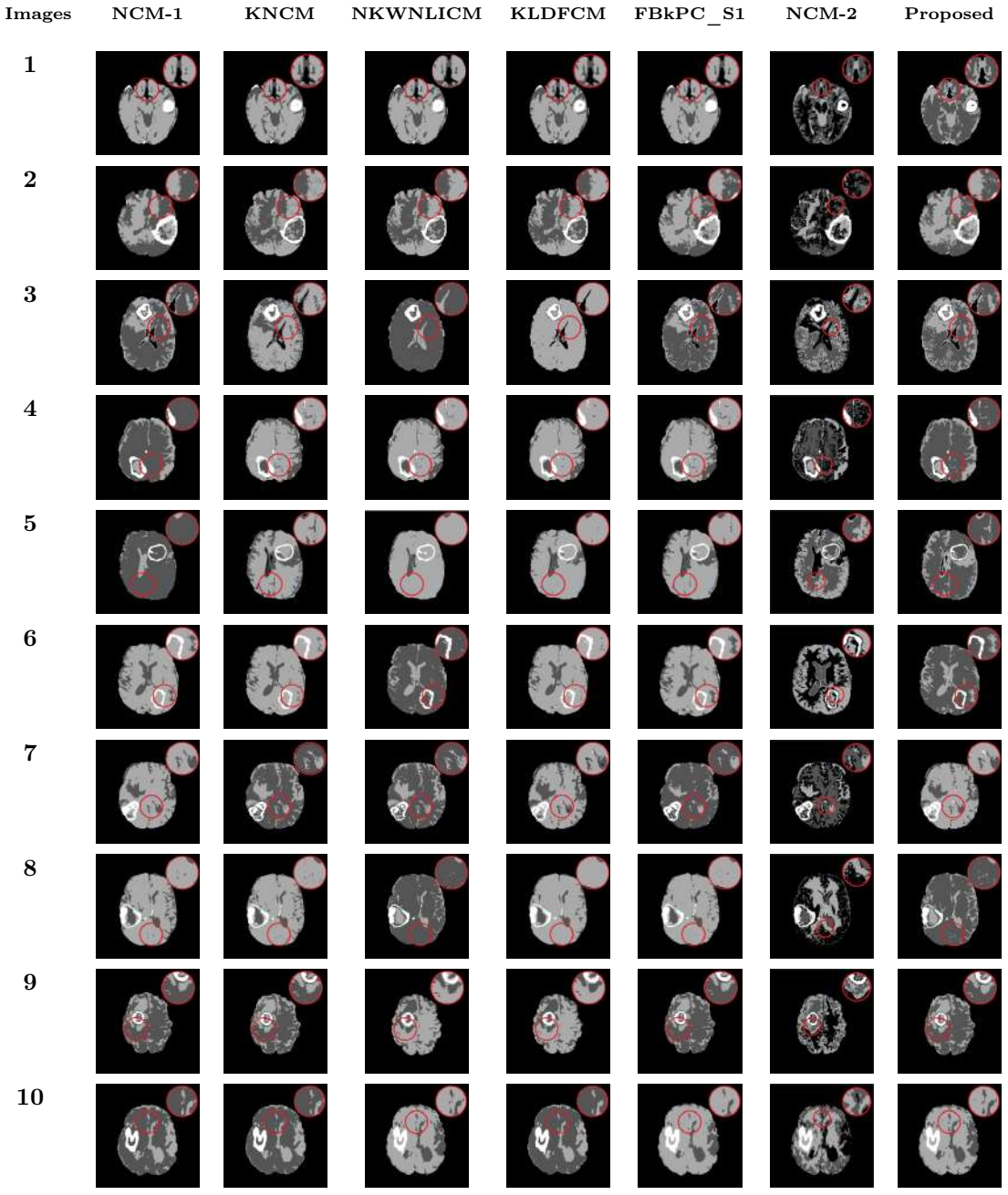

FIGURE 2. Resultant of proposed and comparative state-of-the-art methods.

the segmented results. Figure 2 illustrates the segmentation outcomes for some representative images from the dataset, showcasing the performance of the proposed method alongside other advanced algorithms. To enhance clarity in visual analysis, the segmented regions, particularly the tumor boundaries, are highlighted with red circles. Additionally, zoomed-in views are provided within the same figure to facilitate closer examination of the segmented regions. This dual analysis approach enables a more comprehensive comparison, allowing for a deeper understanding of the strengths and limitations of the proposed method relative to competing techniques. The objective assessment provides a comprehensive quantitative analysis of the proposed method in comparison with several other advanced segmentation techniques, highlighting the strengths and weaknesses of each approach. The NCM-1 algorithm is effective at removing outliers from the image data, ensuring a cleaner dataset for segmentation. However, it exhibits limitations in accurately segmenting the more subtle and complex regions of the brain, particularly in areas where fine details are essential for precise diagnosis. As a result, NCM-1 struggles to capture the intricacies of the tumor boundaries and other smaller internal regions, reducing its overall effectiveness in medical image analysis. KNCM algorithm improves upon NCM-1 by utilizing kernel functions to enhance clustering performance. This enables KNCM to better handle the non-linear and inhomogeneous structures within brain images. While this method shows enhanced clustering capability, its segmentation accuracy is lower than compared to the proposed method. Further, NKWNLICM faces significant challenges in accurately segmenting tumor regions. It fails to effectively distinguish the tumor from surrounding tissues and is notably deficient in segmenting other internal structures within the brain, leading to a lack of overall precision in the segmentation process. While analysing KLDFCM techniques which demonstrates competence in segmenting tumor regions, benefiting from the use of KL divergence to improve clustering in high-dimensional data. However, KLDFCM falls short in

Images	**NCM-1**	**KNCM**	**NKWNLICM**	**KLDFCM**	**FBkPC_S1**	**NCM-2**	**Proposed**
1	0.9287	0.9373	0.9187	0.8394	0.8722	0.8165	**0.9742**
2	0.9228	0.9396	0.8915	0.8508	0.8553	0.8357	**0.9924**
3	0.9169	0.9581	0.9381	0.8404	0.8411	0.8324	**0.9996**
4	0.9241	0.9561	0.9278	0.8716	0.8878	0.8579	**0.9945**
5	0.9240	0.9387	0.9455	0.8971	0.9072	0.8723	**0.9975**
6	0.9239	0.9342	0.9406	0.8739	0.9135	0.8569	**0.9984**
7	0.9295	0.9353	0.9521	0.8675	0.9169	0.8461	**0.9965**
8	0.9328	0.9476	0.9459	0.8648	0.9177	0.8492	**0.9972**
9	0.9345	0.9484	0.9517	0.8971	0.9784	0.8741	**0.9971**
10	0.9132	0.9247	0.9356	0.8523	0.9586	0.8486	**0.9937**

TABLE 1. Values of FPI for the proposed and comparative state-of-the-art methods.

Images	NCM-1	KNCM	NKWNLICM	KLDFCM	FBkPC_S1	NCM-2	Proposed
1	0.0706	0.0613	0.0654	0.1498	0.1537	0.1718	**0.0068**
2	0.0791	0.0744	0.0753	0.1592	0.1820	0.1765	**0.0230**
3	0.0780	0.0648	0.0677	0.1676	0.1579	0.1824	**0.0166**
4	0.0460	0.0363	0.0345	0.1232	0.1210	0.1369	**0.0034**
5	0.0728	0.0524	0.0547	0.1815	0.1375	0.1928	**0.0026**
6	0.0704	0.0618	0.0678	0.1693	0.1364	0.1746	**0.0014**
7	0.0703	0.0602	0.0624	0.1637	0.1354	0.1728	**0.0037**
8	0.0701	0.0637	0.0574	0.1737	0.1632	0.1838	**0.0062**
9	0.0684	0.0547	0.0531	0.1085	0.1055	0.1145	**0.0028**
10	0.0664	0.0513	0.0518	0.1422	0.1325	0.1575	**0.0056**

TABLE 2. Values of MPE for the proposed and comparative state-of-the-art methods.

Images	NCM-1	KNCM	NKWNLICM	KLDFCM	FBkPC_S1	NCM-2	Proposed
1	0.0466	0.0303	0.0229	0.0267	0.0178	0.0298	**0.0143**
2	0.0420	0.0325	0.0270	0.0226	0.0196	0.0263	**0.0168**
3	0.0347	0.0217	0.0198	0.0172	0.0097	0.0192	**0.0066**
4	0.0363	0.0258	0.0214	0.0195	0.0189	0.0211	**0.0132**
5	0.0321	0.0298	0.0275	0.0198	0.0173	0.0229	**0.0112**
6	0.0234	0.0201	0.0195	0.0185	0.0105	0.0198	**0.0072**
7	0.0365	0.0226	0.0231	0.0735	0.1647	0.0846	**0.0169**
8	0.0333	0.0253	0.0226	0.0715	0.0945	0.0810	**0.0126**
9	0.0372	0.0276	0.0234	0.0857	0.0934	0.0921	**0.0111**
10	0.0252	0.0201	0.0195	0.0795	0.0654	0.0846	**0.0050**

TABLE 3. Values of XBI for the proposed and comparative state-of-the-art methods.

Algorithm	Computational time (s)	Number of iteration
NCM-1	6.4247	156
KNCM	8.3589	183
NKWNLICM	5.2194	127
KLDFCM	3.1784	86
FBKPC_S1	4.2488	108
NCM-2	6.7251	162
Proposed	3.24587	79

TABLE 4. Computational time and number of iterations for proposed and other comparative methods.

accurately clustering other non-tumor areas of the brain, leading to incomplete and imprecise segmentation. Moreover, FBkPCS1 technique suffers from imprecision, particularly in defining the boundaries of tumor regions. The method often fails to accurately capture the fine details of the tumor edges, which are crucial for medical diagnosis and treatment planning. On examining the results from NCM-2, it is observed that while the NCM-2 algorithm is capable of segmenting tumor regions to a certain extent, but it does not adequately capture the intricate internal structures of the brain. This limitation often results in degraded segmentation, particularly in regions where tissue boundaries are less distinct, thereby reducing the overall segmentation accuracy and reliability of the method. Furthermore, KLKNCM method outperforms the aforementioned algorithms in multiple aspects. By incorporating kernel-induced clustering with the Neutrosophic c-means framework
and the KL distance measure, the KLKNCM method achieves superior segmentation accuracy. It effectively segments both the tumor regions and other internal structures of the brain, addressing the limitations observed in the other methods. Finally, KLKNCM method provides more precise boundary delineation and improved differentiation of inhomogeneous brain tissues. Furthermore, it offers enhanced computational efficiency, making it a highly effective and practical solution for brain tumor segmentation in clinical settings.

Meanwhile, the evaluation of the proposed method is further supported by an analysis of cluster validation metrics, with the results summarized in Tables 1-3. The optimal values for each metric are highlighted in bold for clarity. Upon reviewing the cluster validation results, it is evident that FPI for the proposed KLKNCM technique is significantly higher compared to the other methods. A higher FPI value indicates greater correctness and precision in the clustering process, demonstrating the ability of KLKNCM to accurately segment complex brain structures. Furthermore, MPE and XBI values
for the KLKNCM method are lower in comparison to those of the alternative clustering algorithms. Lower values of MPE and XBI indicate more distinct and well-separated clusters, which further affirms the accuracy and effectiveness of the proposed technique. These lower indices suggest that the KLKNCM method not only achieves better clustering precision but also minimizes overlap between clusters, ensuring more accurate segmentation of brain regions. In summary, the superior performance of the proposed KLKNCM method across these validation metrics, particularly with respect to FPI, MPE, and XBI, highlights its effectiveness and supremacy over the other state-of-the-art techniques. This analysis underscores the robustness and efficiency of the KLKNCM algorithm in achieving highly accurate and computationally efficient brain tumor segmentation.

In addition, the comparative analysis of the proposed algorithm with other state-of-the-art clustering methods highlights its superior efficiency in terms of both computational time and

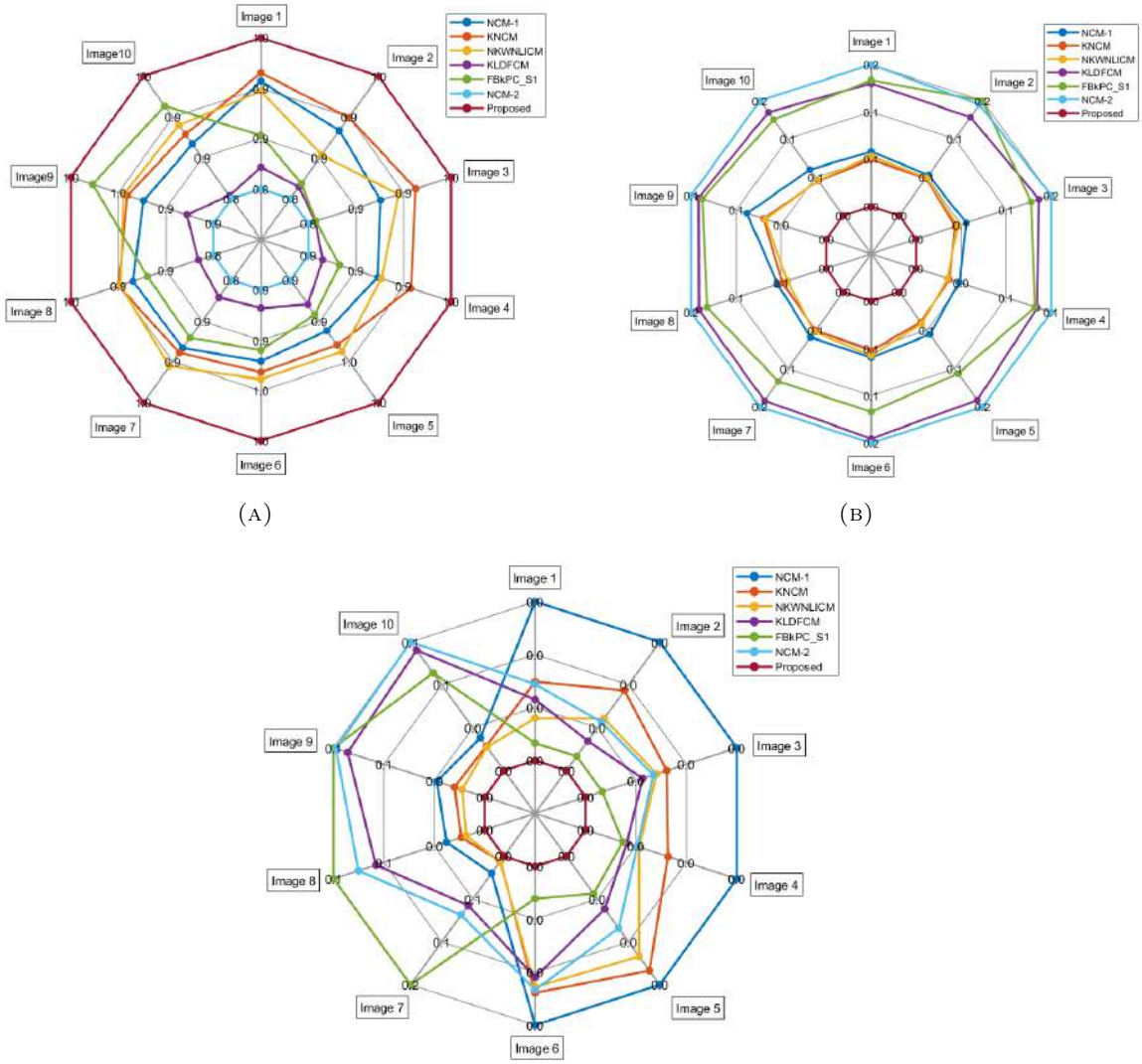

FIGURE 3. Graphical representation of quality assessment metrics (a) Quality assessment through FPI, (b) Quality assessment through MPE, (c) Quality assessment through XBI.

iteration count which is given in the Table 4. The proposed algorithm demonstrates a competitive computational time, indicating its capability to handle clustering tasks with minimal resource consumption. Furthermore, the number of iterations required for convergence is significantly lower in the proposed method compared to the other algorithms. This reduction in iteration count underscores the KLKNCM has the enhanced convergence speed, which is crucial for minimizing computational overhead in iterative clustering processes. The iterative nature of clustering algorithms often poses a challenge in balancing accuracy and efficiency;

however, the proposed method effectively addresses this by achieving rapid convergence without compromising performance. Moreover, the graph where plotted to show the efficiency of the proposed algorithm and it displayed in Figure 3. Altogether, the results suggest that the proposed algorithm not only reduces the computational burden but also accelerates the clustering process, making it a suitable choice for applications where both time efficiency and processing power are limited. In conclusion, the proposed algorithm outperforms the comparative methods by demonstrating a balance between computational efficiency and iteration reduction, thereby providing an effective solution for real-world clustering applications.

7. **Limitation and Future Research**

While the proposed method demonstrates the superior performance, but still there persists certain limitations. Even though, integration of the kernel distance and KL divergence in NCM elevates the segmentation accuracy, the developed method still depends on the parameter tuning, which impacts the robustness of the method. Added to this, the evaluation has been done on benchmark datasets but the performance across large-scale with diverse datasets yet to be comprehensively validated. These limitations naturally point toward several directions for future research, incorporating deep learning frameworks such as CNN with the proposed framework could maximize the benefits data-driven learning to achieve the superior accuracy. Automated parameter optimization techniques also represent a valuable extension, reducing the reliance on manual tuning and improving reproducibility. Furthermore, expanding the approach to handle multi-class segmentation of tumor sub-regions and applying it to other neurological disorders would broaden its clinical relevance.

8. **Conclusion**

This study introduced a novel KLKNCM technique for the segmentation of brain tumors. The proposed approach effectively addresses the challenges posed by the non-linear and inhomogeneous nature of brain structures, providing accurate segmentation while minimizing computational overhead. The proposed method has been rigorously tested against five other state-of-the-art clustering algorithms, with its performance validated through both objective metrics and subjective assessments. The results highlight the superiority of our approach in terms of segmentation accuracy, computational cost, and robustness, demonstrating its potential for practical use in clinical settings. Further, parameters of the algorithm were examined in depth to demonstrate their functions in the segmentation methodology. In addition, runtime calculations and iteration analysis were carried out in order to acquire a comprehensive understanding of the results. In future, the proposed approach will be used to classify medical images based on segmentation.

Funding: This research was funded byUniversity Grants Commission (UGC), Department of Higher Education, Government of India through SJSGC Fellowship vide UGC scholarship ID No. 202223-UGCES-22-OB-TAM-F-SJSGC-9475.

Data availability: Enquiries about data availability should be directed to the authors.

Conflicts of Interest: Declare conflicts of interest or state "The authors declare no conflict of interest.

Ethical approval This article does not contain any studies with human participants performed by any of the authors.

References

1. Preetha, R., Priyadarsini, M. J. P., & Nisha, J. S. (2024). Automated brain tumor detection from magnetic resonance images using fine-tuned EfficientNet-B4 convolutional neural network. IEEE Access, 12, 112181-112195.
2. Adams, L. C., Bressem, K. K., Ziegeler, K., Vahldiek, J. L., & Poddubnyy, D. (2024). Artificial intelligence to analyze magnetic resonance imaging in rheumatology. Joint Bone Spine, 91(3), 105651.
3. Ranjbarzadeh, R., Zarbakhsh, P., Caputo, A., Tirkolaee, E. B., & Bendechache, M. (2024). Brain tumor segmentation based on optimized convolutional neural network and improved chimp optimization algorithm. Computers in Biology and Medicine, 168, 107723.
4. Akbar, A. S., Fatichah, C., Suciati, N., & ZaâĂŹin, C. (2024). Yaru3DFPN: a lightweight modified 3D UNet with feature pyramid network and combine thresholding for brain tumor segmentation. Neural Computing and Applications, 36(13), 7529-7544.
5. Biratu, E. S., Schwenker, F., Debelee, T. G., Kebede, S. R., Negera, W. G., & Molla, H. T. (2021). Enhanced region growing for brain tumor MR image segmentation. Journal of Imaging, 7(2), 22.
6. Annavarapu, A., & Borra, S. (2024). An adaptive watershed segmentation based medical image denoising using deep convolutional neural networks. Biomedical Signal Processing and Control, 93, 106119.
7. Halder, A., & Talukdar, N. A. (2024). Kernel induced semi-supervised spatial clustering: a novel brain MRI segmentation technique. Multimedia Tools and Applications, 83(16), 49213-49241.
8. Ganapathy, S., Thoidingjam, V., & Sen, A. (2024). A brain tumor prediction system for detecting the tumor disease using mini batch k-means clustering and cnn. Multimedia Tools and Applications, 83(35), 83053-83091.
9. Xu, M., Guo, L., & Wu, H. C. (2024). Novel robust automatic brain-tumor detection and segmentation using magnetic resonance imaging. IEEE Sensors Journal, 24(7), 10957-10964.
10. Nandhini, M., Dhanalakshmi, P., & Lavanya, K. G. (2024). A soft clustering approach for segmenting brain tumor in intuitionistic fuzzy environment. Biomedical Signal Processing and Control, 91, 105996.
11. Bezdek, J. C., Ehrlich, R., & Full, W. (1984). FCM: The fuzzy c-means clustering algorithm. Computers & geosciences, 10(2-3), 191-203.
12. IRFAN, M., RAHMAN, S., JALALAH, M., ALMAWGANI, A. H., & ELJAK, L. A. B. (2024). Improved Brain Tumor Segmentation and Classification in Brain MRI With FCM-SVM: A Diagnostic Approach.
13. Jafrasteh, B., LubiÃąn-GutiÃĺrrez, M., LubiÃąn-LÃşpez, S. P., & Benavente-FernÃąndez, I. (2024). Enhanced spatial Fuzzy C-Means algorithm for brain tissue segmentation in T1 images. Neuroinformatics, 22(4), 407-420.

14. Kouhi, A., Seyedarabi, H., & Aghagolzadeh, A. (2020). Robust FCM clustering algorithm with combined spatial constraint and membership matrix local information for brain MRI segmentation. Expert Systems with Applications, 146, 113159.
15. Kaushal, M., Danish Lohani, Q. M., & Castillo, O. (2024). Weighted intuitionistic fuzzy c-means clustering algorithms. International Journal of Fuzzy Systems, 26(3), 943-977.
16. Lavanya, K. G., Dhanalakshmi, P., & Nandhini, M. (2024). A novel enhancement-based rapid kernel-induced intuitionistic fuzzy c-means clustering for brain tumor image: KG Lavanya et al. Soft Computing, 28(9), 6657-6670.
17. Smarandache, F. (1998). Neutrosophy: neutrosophic probability, set, and logic: analytic synthesis & synthetic analysis.
18. Guo, Y., & Sengur, A. (2015). NCM: Neutrosophic c-means clustering algorithm. Pattern Recognition, 48(8), 2710-2724.
19. Akbulut, Y., ÅđengÃijr, A., Guo, Y., & Polat, K. (2017). KNCM: Kernel neutrosophic c-means clustering. Applied Soft Computing, 52, 714-724.
20. Singh, P. (2020). A neutrosophic-entropy based clustering algorithm (NEBCA) with HSV color system: A special application in segmentation of ParkinsonâĂŹs disease (PD) MR images. Computer methods and programs in biomedicine, 189, 105317.
21. Gharieb, R. R., Gendy, G., Abdelfattah, A., & Selim, H. (2017). Adaptive local data and membership based KL divergence incorporating C-means algorithm for fuzzy image segmentation. Applied Soft Computing, 59, 143-152.
22. Gharieb, R. R., & Gendy, G. (2014, December). Fuzzy C-means with a local membership KL distance for medical image segmentation. In 2014 Cairo International Biomedical Engineering Conference (CIBEC) (pp. 47-50). IEEE.
23. Lu, Z., Qiu, Y.,& Zhan, T. (2019). Neutrosophic C-means clustering with local information and noise distance-based kernel metric image segmentation. Journal of Visual Communication and Image Representation, 58, 269-276.
24. Wang, C., Pedrycz, W., Li, Z., & Zhou, M. (2021). KullbackâĂŞLeibler divergence-based fuzzy C-means clustering incorporating morphological reconstruction and wavelet frames for image segmentation. IEEE Transactions on cybernetics, 52(8), 7612-7623.
25. Kumar, P., Agrawal, R. K., & Kumar, D. (2023). Fast and robust spatial fuzzy bounded k-plane clustering method for human brain MRI image segmentation. Applied Soft Computing, 133, 109939.
26. Farooq, A., & Memon, K. H. (2024). Kernel possibilistic fuzzy c-means clustering algorithm based on morphological reconstruction and membership filtering. Fuzzy Sets and Systems, 477, 108792.
27. Bakas, S., Akbari, H., Sotiras, A., Bilello, M., Rozycki, M., Kirby, J. S., ... & Davatzikos, C. (2017). Advancing the cancer genome atlas glioma MRI collections with expert segmentation labels and radiomic features. Scientific data, 4(1), 170117.
28. Chaira, T. (2022). Neutrosophic set based clustering approach for segmenting abnormal regions in mammogram images. Soft Computing, 26(19), 10423-10433.
29. Ryoo, J. H., Park, S., Kim, S., & Ryoo, H. S. (2020). Efficiency of cluster validity indexes in fuzzy clusterwise generalized structured component analysis. Symmetry, 12(9), 1514.
30. Liu, Y., Zhang, X., Chen, J., & Chao, H. (2019). A validity index for fuzzy clustering based on bipartite modularity. Journal of Electrical and Computer Engineering, 2019(1), 2719617.
31. Kaushal, M., & Lohani, Q. D. (2022). Generalized intuitionistic fuzzy c-means clustering algorithm using an adaptive intuitionistic fuzzification technique. Granular Computing, 7(1), 183-195.

Received: Aug 9, 2025. Accepted: Feb 15, 2026